A R C H I V E S O F M E T A L L U R G Y A N D M A T E R I A L S
Volume 57 2012 Issue 1
DOI: 10.2478/v10172-011-0153-2

S. SAWICKI*, H. DYJA*

THEORETICAL AND EXPERIMENTAL ANALYSIS OF THE BIMETALLIC RIBBED BARS STEEL – STEEL RESISTANT TO CORROSION ROLLING PROCESS

TEORETYCZNA I DOŚWIADCZALNA ANALIZA WYTWARZANIA BIMETALOWYCH PRĘTÓW ŻEBROWANYCH STAL – STAL ODPORNA NA KOROZJĘ

The paper presents results of theoretical and experimental studies on the process of rolling bimetallic ribbed bars in the finishing pass. The work has determined the effect of the shape of oval preformed strip with a variable clad layer share on the distribution of clad layer thickness in bimetallic ribbed bars rolled in the finishing pass. The theoretical and experimental studies were carried out with the aim of determining the clad layer thickness that will ensure the appropriate corrosion resistance of finished product. A software application, Forge2007®, was used for numerical modeling.

Keywords: FEM, bimetallic bars, steel-steel resistant to corrosion, hot rolling, numerical modelling, ribbed bars

W pracy przedstawiono wyniki badań teoretycznych i doświadczalnych procesu walcowania prętów żebrowanych bimetalowych w wykroju gotowym. W pracy określono wpływ kształtu pasma owalnego przedgotowego o różnym udziale warstwy platerującej na rozkład grubości warstwy platerującej w prętach żebrowanych bimetalowych walcowanych w wykroju gotowym. Teoretyczne i doświadczalne badania przeprowadzono w celu określenia grubości warstwy platerującej zapewniającej odpowiednią odporność na korozję gotowego wyrobu. Do modelowania numerycznego wykorzystano program komputerowy Forge2007®.

1. Introduction

A considerable increase in interest in using corrosion resistant steel clad ribbed bars in the construction industry has been observed in recent years. This is owing to the particular properties of these bars, namely high durability and rigidity, good mechanical properties, and high corrosion resistance.

A properly designed rolling process should ensure that a clad layer of the proper and even thickness is obtained on the perimeter and along the length of the bar, which will not break in the finishing pass. Moreover, the shape of the finishing pass should be designed in such a manner as to prevent any surface defects of the clad layer from forming in it during forming ribs on the bar.

Theoretical and experimental studies on the process of rolling bimetallic ribbed bars, where the core was of the constructional carbon steel C45E and the clad layer was made of the corrosion resistant steel X2CrNi18-10, were carried out within the work. To produce the feedstock, which was round bimetallic bar, the explosive welding method was used. This method ensures that bimetallic feedstock with the high strength and good mechanical properties of the joint between the core and the clad layer will be obtained [1, 2, 8, 9-15]. The rolling of ribbed bars was carried out on a D150 two-high laboratory mill.

2. Materials used for research

The accuracy of calculations performed using a computer program is dependent on the accurate determination of the properties of materials used for tests. Undertaken experimental studies aimed at the determining the effect of strain parameters on the magnitude of yield stress for steel C45E and for steel X2CrNi18-10. Plastometric tests were performed on a Gleeble 3800 plastometer owned by the Institute of Modelling and Automation of Plastic Working Processes, using strain rates of $0.1s^{-1}$, $1.0s^{-1}$ and $10s^{-1}$ respectively. Chemical composition of materials used for tests is given in

* CZESTOCHOWA UNIVERSITY OF TECHNOLOGY, FACULTY OF MATERIALS PROCESSING TECHNOLOGY AND APPLIED PHYSICS, 42-200 CZESTOCHOWA, 19 ARMII KRAJOWEJ AL., POLAND

TABLE 1

Chemical composition of materials used for tests [%]

Steel	C	Mn	Si	P	S	Cr	Ni	Mo	Cu	Sn
C45E	0.45	0.64	0.21	0.015	0.031	0.13	0.14	0.04	0.25	0.015
X2CrNi18-10	0.03	2.00	0.24	0.045	0.03	19.0	10.0	0.75	–	–

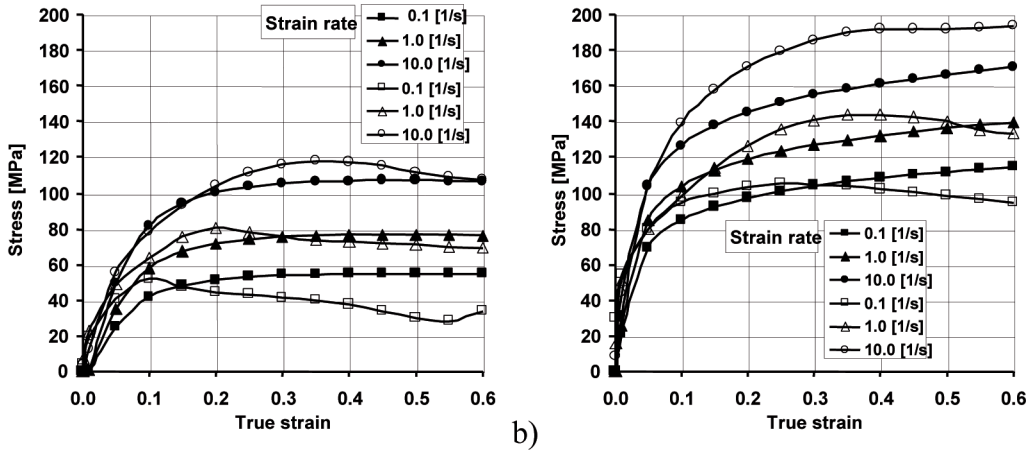

Fig. 1. Example flow curves for: a) steel C45E and b) for steel X2CrNi18-10, at temperature of 1100°C, (the curves denoted with filled signs represent experimental results, the remaining curves are approximated based on experimental tests)

Table 1, whereas Fig. 1 illustrates the example testing results in the form of flow curves for steel C45E and for steel X2CrNi18-10.

When analyzing the data in Figure 1 it can be found that the yield stress values for the X2CrNi18-10 steel are much higher than for the C45E steel. This difference has a considerable influence on the process of rolling bimetallic bars in passes. The higher yield stress values in the clad layer reduce the effect of the clad layer "flowing down" from the bimetallic bar core [3, 4].

In order to obtain a mathematical relationship making the value of flow stress, σ_p, dependent on deformation parameters, (ε, $\dot{\varepsilon}$, T), the results of the performed tests were approximate to a functional relationship described by Equation (1). The flow stress σ_p dependence of strain intensity ε, strain rate $\dot{\varepsilon}$ and temperature T for the C45E steel and for the X2CrNi18-10 steel are approximated by Henzel-Spittel formula expressed as [6]:

$$\sigma_p = A_0 \exp^{m_1 T} \varepsilon^{m_2} \dot{\varepsilon}^{m_3} \exp^{m_4 \varepsilon} \qquad (1)$$

The coefficients *A0*, *m1*, *m2*, *m3*, *m4* of the C45E steel and the X2CrNi18-10 steel are given in Table 2.

TABLE 2

Parameters of function (1) for the C45E steel and for the X2CrNi18-10 steel

Steel	*A0*	*m1*	*m2*	*m3*	*m4*
C45E	1521.3	– 0.00269	– 0.12651	0.14542	– 0.05957
X2CrNi18-10	4321.6	– 0.00305	0.10835	0.08647	– 0.01270

3. Explosive welding of bimetallic stock

For explosive welding of bars, sets composed of X2CrNi18-10 corrosion-resisting steel pipes and C45E steel bars were prepared. The system and its individual components are illustrated in Fig. 2 [7, 11]. Whereas, Figure 3 shows finished bimetallic bars obtained after explosive welding. Based on the testing of bimetallic bars after explosive welding it has been found that by changing the initial dimensions of pipes and bars and the initial distances between them, bimetallic bars of the desired inner diameter and the required cladding layer thickness can be obtained.

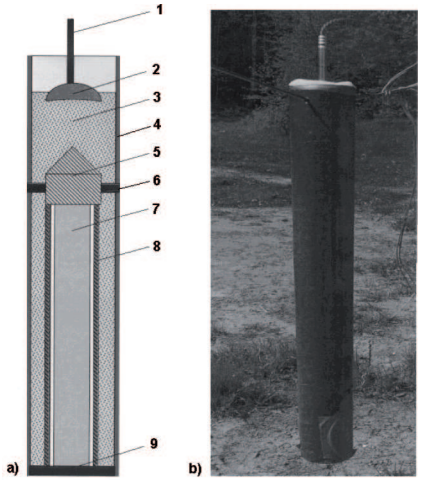

Fig. 2. Schematic (a) and actual view (b) of systems used for explosive welding of bimetallic stock: 1 – detonator, 2 – primary explosive, 3 – loose explosive, 4 – PCV tube, 5 – centring plug, 6 – element aligning the system in the container, 7 – steel bar, 8 – corrosion-resisting steel pipe, 9 – bottom centring disk

Fig. 3. Bimetallic bars after explosive welding

4. Microstructure of the joint zone in bimetallic bars after explosive welding

Samples for microstructural examinations were taken from bimetallic bars obtained after explosive welding. The analysis of changes in the microstructure was performed both for the core and for the clad layer. Figure 4 a and 4b show the microstructure of the joint regions in the bars examined. It was found that the core after explosive welding exhibited a ferritic-pearlitic structure (with a majority of pearlite of approx. 80%) with the ferrite grain size in the standard class of 9.0, and the pearlite grain size of 8.0÷8.5 (acc. to the EN-ISO 643:2003 standard). At the joint zone, pearlite grains were in the standard class of 8.0, whereas the ferrite grains in the standard class of 9.0 (acc. to the EN-ISO 643:2003 standard). The clad layer, in turn, had an austenitic structure with the grain size in the standard class of 9.0. It was found that the area of the core-clad layer joint was wavy, with no oxides or fraying. No presence of any impurities was found in this zone.

The analysis of the presented testing results shows that different bars after explosive welding exhibited comparable cladding layer and core structures in the joint region. No differences in grain sizes between ferrite and pearlite were observed. A wavy joint area was found to occur in both cases.

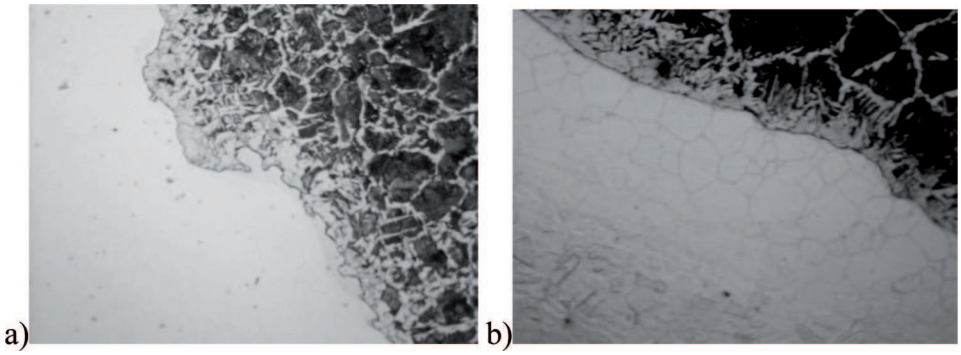

Fig. 4. The microstructure in the joint region of a bimetallic bar after explosive welding: a) – the core, zoom 100x, etched with Nital; b) – clad layer, zoom 100x, etched with 45ml H2O, 30ml HNO3, 15ml HCl, 10ml HF

5. The quality of the bimetallic bar bond joint

For the quality assessment of bimetallic bars, a method relying on the maximum shearing stress at the joint boundary was used. The results of the quality examination of the steel – corrosion-resisting steel joint (maximal shearing stress) after explosive welding are represented in Figure 5. The data in Figure 5 show that the difference between the lowest (test piece no. 2; 140 MPa) and the highest (test piece no. 3; 230 MPa) stress values does not exceed 40%. For all of the test pieces examined, the quality of the joint was good enough so that no breaking of individual layers occurred, but only squeezing out of the bimetallic bar through the test die.

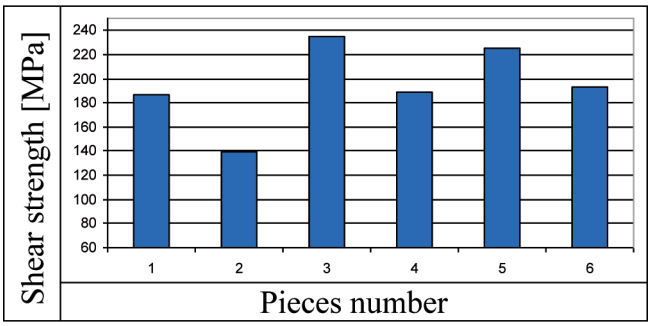

Fig. 5. The shear strength of bimetallic test pieces after explosive welding

To examine the quality of the joint between bimetallic layers more precisely, microanalysis of the joint region was made by the EDX method. The results of this microanalysis are given in Figures 6 and in Table 3.

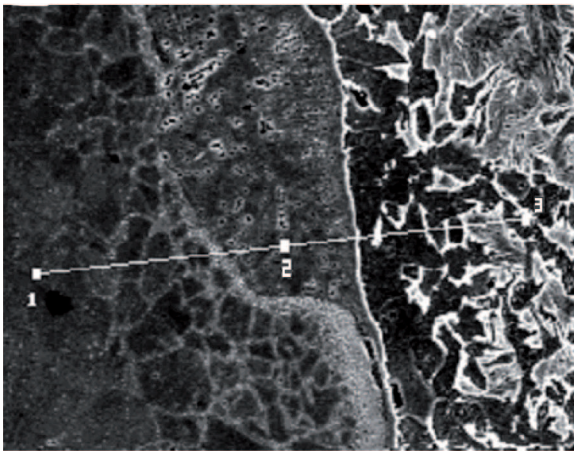

Fig. 6. The microstructure of the joint region of bimetallic bar after explosive welding, zoom 320x – EDX analysis

From the results of the EDX analysis of a bimetallic sample after explosive welding it can be found that locally, at the joint boundary, a 35 μm wide transitory film has formed – region 2, which consist of a mixture of mainly nickel, chromium and iron, with the following contents: 10% Cr, 5% Ni and 83% Fe. For region 1 – the core of the bimetallic sample, the contents of these elements are as follows: 0% Cr, 0% Ni and 99% Fe; whereas, in region 3 – the clad layer, these are: 19% Cr, 10% Ni and 69% Fe.

TABLE 3
Percentage fractions of elements in particular regions of the joint from Figure 6 [wt%/at%]

Area	Si	Mn	Fe	Cr	Ni
1	0.27/0.53	0.66/0.67	99.07/98.80	–	–
2	0.48/0.95	1.17/1.18	83.08/82.27	10.00/10.64	5.27/4.96
3	0.58/1.14	1.73/1.74	68.68/67.66	18.85/19.95	10.15/9.51

Microhardness tests of layers in respective joint regions were carried out for 3 selected samples obtained after explosive welding. The results of these tests are represented in Figure 7. The hardness tests were performed by the Vickers method according to the PN-ISO 6507-3 standard.

When comparing the obtained microhardness values for the initial materials and the bimetallic bars after explosive welding it can be found that an increase in the microhardness of the materials examined has occurred. This microhardness increase was caused by hardening of the material during explosive welding and the deformation of the clad layer. A high increase in microhardness was observed in the joint zone. The highest microhardness increase in the joint zone (25% to 30%) was obtained for a bimetallic sample, which had a clad layer thickness of 1.0mm (Fig. 7a). In the bimetallic sample, in which the clad layer thickness was 1.5 mm, the microhardness increase in the joint zone was smaller, ranging from 20% to 25% (Fig. 7b). With the clad layer thickness of 2.0 mm, the microhardness increase in the joint zone ranged from 15% to 20% (Fig. 7c).

The microhardness increment for steel C45E explosively welded averaged out at about 5%. The increment in the microhardness of the clad layer after explosive welding was approx. 10% on the average. Microhardness values for homogeneous materials were, respectively: for steel C45E, an average of 282 HV0.1; while for the corrosion-resisting steel, 305 HV0.1 on the average.

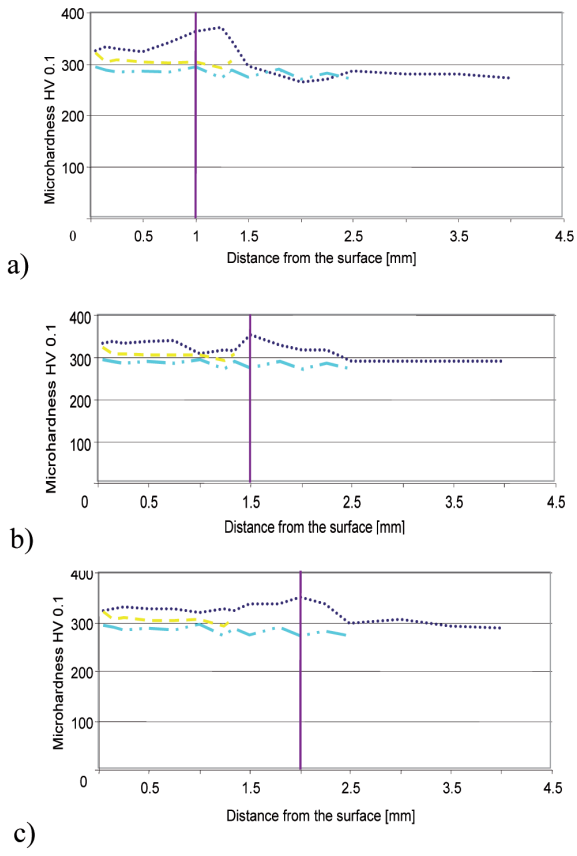

Fig. 7. The distribution of microhardness for stock materials and in bimetallic bars after explosive welding: with a clad layer thickness of: a) – 1.0 mm; b) – 1.5 mm; c) – 2.0 mm

6. Initial conditions applied during theoretical examinations and experimental tests

The following initial parameters were taken for rolling procecs simulation: a roll diameter of 150 mm; the temperature of rolled bimetallic strip was assumed to be uniform within the whole strip volume and equal to 1100°C; the rolling speed equal to 0.5 m/s; and a friction factor of 0.7. The nodes of both grids were shared.

These conditions were selected so that it was possible to verify the theoretical results in experimental tests in the Rolling Laboratory of the Institute for the Modelling and Automation of Plastic Working Processes.

For the experimental tests and theoretical studies, bimetallic feedstock in the form of 22mm-diameter round bars made by the explosive method was used, in which the share of the clad layer on the bar cross-section was approx. 17.4%, 25.7% and 33.2%, respectively.

The junction between the core and the cladding layer was defined as closely fitting. The nodes of both grids were shared.

In order to determine the effect of clad layer thickness on the correct formation of ribs in finished bars, numerical simulations of the process of rolling 18 mm-diameter bimetallic bars in the preforming and the finishing passes were performed. The round bimetallic feedstock rolling process was conducted in the flat oval preforming pass. The shape of the preforming pass (Fig. 8) had been designed following the rules provided in literature [2, 7, 15].

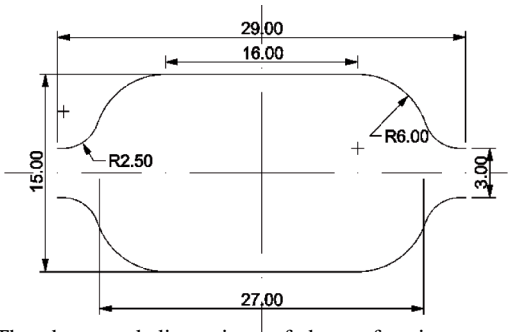

Fig. 8. The shape and dimensions of the preforming pass used in rolling

The shape and dimensions of the finishing ribbed pass had been designed based on the standards for finished ribbed bars [16, 17].

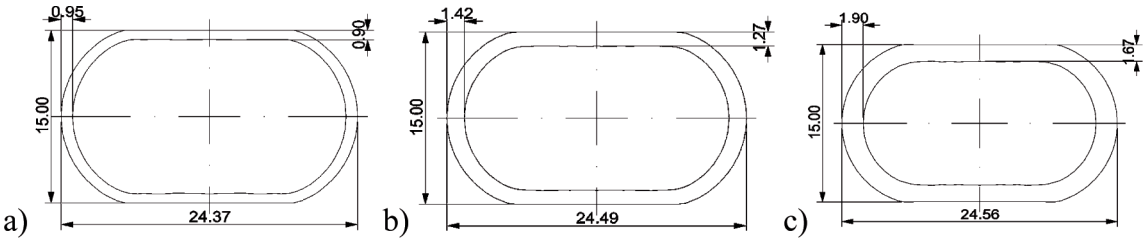

Fig. 9. The shape and dimensions of bimetallic preformed strip obtained from the theoretical examination of the process of rolling in the flat oval pass with the clad layer thickness fraction of the bimetallic stock equal to, respectively: a) 17.4%, b) 25.7%, c) 33.2%

7. Examination results and their analysis

On the basis of the results of computer simulations of bimetallic ribbed bar rolling in the preforming and the finished passes, distributions of clad layer thickness over the rolled bar cross-section for the preforming pass, and over the longitudinal section for the finishing pass were made.

Figure 9 shows the shape and dimensions of bimetallic strips obtained from the numerical simulations of the process of bimetallic feedstock rolling in the flat oval-preforming pass.

The dimensions of oval bimetallic strips after rolling in the preforming pass are summarised in Table 4.

Based on the data shown in Fig. 9 and in Table 4 it can be stated that the share of the clad layer on the cross-section of the bimetallic strip during rolling the bimetallic feedstock in the flat oval-preforming pass has significantly decreased. During rolling in the flat oval pass the clad layer share in the strip cross-section decreased by about 0.5÷1.0%.

TABLE 4
Numerical examination results obtained from the simulation of the process of rolling bimetallic strip in the flat oval pass

Thickness of the clad layer [mm]	Percentage of the outer layer [%]		Dimensions of the strip [mm]	
	Bimetallic bars	After rolling in the preforming pass	Height bimetallic stock	Width bimetallic stock
1.00	17.4	17.3	15.00	24.37
1.50	25.7	25.5	15.00	24.49
2.00	33.2	33.1	15.00	24.56

Figure 10 shows the shape of a bimetallic ribbed bar obtained from the computer simulation of the process of finishing-pass rolling of transverse flat oval-shaped feedstock with a clad layer share of 17.3; 25.5; and 33.1 %, respectively.

In bimetallic bars with the outer layer share of 17.3% (Fig. 10a), the thickness of the clad layer in sections between the rib was about 0.70 mm, and at the rib top, 0.81 mm. A smaller clad layer thickness was observed at the rib base. The thickness of the clad layer on the rolling gap entry side was smaller, amounting to 0.48 mm, whereas the layer thickness on the other rib side was greater, being equal to 0.58 mm.

In the case, where the clad layer share in the bimetallic feedstock was 25.5% (Fig. 10b), after rolling in the finishing pass, the thickness of this layer at the rib top was approx. 1.17 mm. The thickness of the clad layer between ribs averaged out at 1.08 mm. The thickness of the clad layer at the rib base was 0.70 mm and 1.04 mm, respectively. In the case of rolling bars with the clad layer share of 33.1% (Fig. 10c), the average outer layer thickness was smaller, amounting to approx. 1.61 mm between ribs, and about 1.65 mm at the rib top. The layer thickness at the rib base for this share was 1.20 mm and 1.39 mm, respectively.

The occurrence of differences in clad layer thickness at the rib base between the both rib sides is due to the mode of rib formation in the roll gap. Figure 11 shows the formation of ribs in the initial zone of the roll gap. During the rolling of oval bimetallic feedstock in the finished ribbed pass, the ribs are formed by filling the pass grooves. Due to the fact that the deformation resistance of the core is high, and a free space exists in the rib groove, the clad layer moves in this particular direction, causing a reduction of clad layer thickness at the rib base.

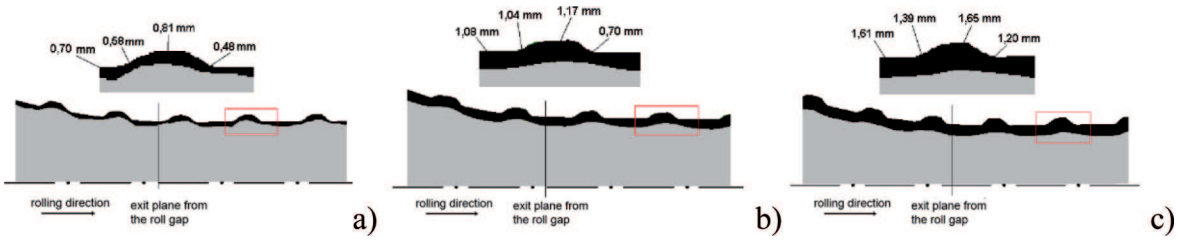

Fig. 10. Distribution of layer surface thickness on the longitudinal cross in deformation zone during bimetallic bar rolling using flat oval pass with the platter layer containing: a) 17.3 %; b) 25.5 %; c) 33.1 %

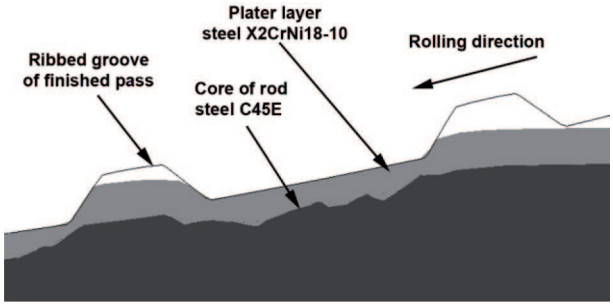

Fig. 11. Forming of the bimetallic round bar ribs in the finishing groove

When analysing the obtained results it can be found that the bimetallic ribbed bar obtained from the transverse flat oval-shaped preformed feedstock shows correct outer dimensions and a correct rib height.

In order to verify the results of the theoretical analysis of the finished-pass ribbed bar rolling process, experimental tests were carried out in laboratory conditions.

For rolling bimetallic ribbed bars, rolls with grooves turned on them were used, which, upon assembly, made a flat oval preforming pass, a single-radial oval preforming pass, and a finishing pass, respectively.

Fig. 12. Laboratory rolls Ø150 mm – general view

As a result of rolling in the preforming pass, an oval strip was obtained (Fig. 13), which was then the feedstock for rolling in the finishing ribbed pass.

Fig. 13. View of a sample preformed oval strip designed for rolling 18 mm-diameter ribbed bars

As a result of oval preformed strip rolling in the finishing pass, bimetallic ribbed bars were obtained. Figure 14 shows sample shapes of bimetallic ribbed bars obtained in the process of rolling on the D150 laboratory mill.

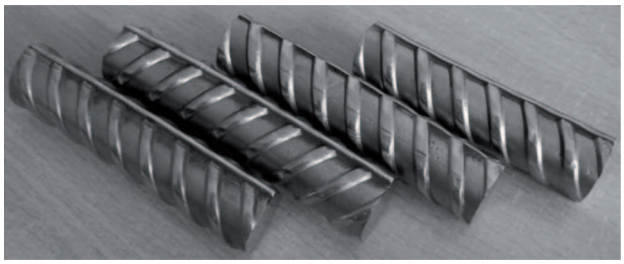

Fig. 14. Bimetallic ribbed round bars

At the next stage of the work, the effect of the shape of oval preformed strip with a different clad layer share on the distribution of clad layer thickness in bars rolled on the D150 two-high mill was determined. Samples were taken from the bimetallic strips after rolling to perform the analysis of clad layer thickness. The samples taken were slit lengthwise and microsections were made. After the microsections had been prepared, digital pictures of the surfaces to be examined were made. Figure 15 show the pictures of the microsections made on bimetallic bars with a different thickness of the clad layer.

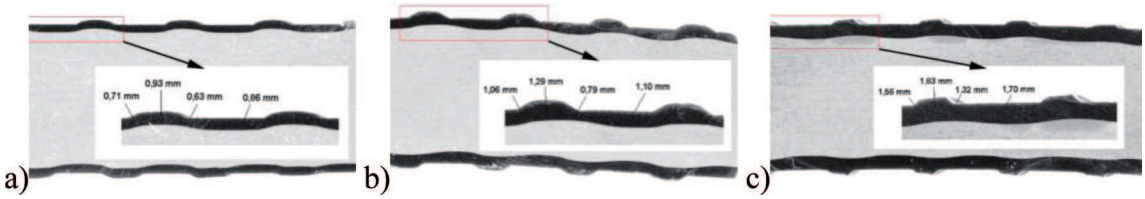

Fig. 15. Distribution of layer surface thickness on the longitudinal section in deformation zone during bimetallic bar rolling using flat oval pass with the platter layer containing: a) 17.3 %; b) 25.5 %; c) 33.1 %

During the rolling of bimetallic bars from feedstock with the clad layer share equal to 17.3% (Fig. 15a), the thickness of the clad layer in sections between ribs on finished bars was on average 0.86 mm. At the rib top, the layer was 0.93 mm thick. A smaller clad layer thickness was found at the rib base. The thickness of that layer was variable, depending on the rolling direction. At the rib base on the side opposite to the rolling direction, the clad layer thickness was 0.71 mm. On the other rib side, the layer thickness was smaller, being 0.63 mm.

In the case, where the feedstock of the clad layer share of 25.5% (Fig. 15b) was used for rolling, the clad layer thickness between ribs on finished bars was found to be 1.10 mm on average. At the rib top, the layer was thicker (1.29 mm thick). At the rib base, similarly as before, the clad layer thickness on the side opposite to the rolling direction was smaller at the top, being equal on average to 1.06 mm. On the other rib side, the layer thickness was even smaller, amounting to approx. 0.79 mm.

For ribs obtained from the feedstock with the clad layer share of 33.1% (Fig. 15c), the clad layer thickness between ribs was approx. 1.70 mm. At the rib top, the layer thickness was bigger (1.83 mm). The clad layer has a smaller thickness at the rib base. On the side opposite to the rolling direction, it averaged out at about 1.56 mm. On the other rib side, the layer thickness was smaller, being 1.32 mm.

8. Conclusions

On the basis of the performed tests it was found that by the proper selection of explosive welding parameters for the metals tested, a bimetallic semi-finished product was obtained, which was characterized by a fast joint between bimetallic layers with regular waves, meeting the conditions imposed on feedstock to be hot rolled. The good quality of the joint between the bimetallic layers is indicated by the existence of a transitory layer between the bimetallic feedstock layers joined.

Theoretical and experimental studies on the process of rolling ribbed bars from C45E steels clad with the X2CrNi18-10 corrosion-resisting steel in the finishing pass were carried out within the work. By comparing the process of rolling bimetallic bars from feedstock with a different share of the clad layer using the oval preforming pass of different shape it could be found that, for all thicknesses of the clad layer on the feedstock, a finished product in the form of ribbed bimetallic bar was obtained, which was free from any laps and breaks of the clad layer on the bimetallic bar surface.

During the rolling of bars from the flat oval bimetallic feedstock, ribbed bars of the proper shape and the correct height of individual ribs were obtained. The use of flat oval strips, as preformed strips, makes it possible to obtain a larger rib height and a better fill of the finished pass groove elements during rolling of bars in the finished ribbed pass.

REFERENCES

[1] S. B e r s k i, Z. S t r a d o m s k i, H. D y j a, Quality of bimetal Al-Cu joint after explosive cladding, Journal of Achievements in Materials and Manufacturing Engineering **22**, 1, 73-76 (2007).
[2] H. D y j a, S. M r ó z, D. R y d z, Technology and modelling the processes of rolling of bimetal articles. Publishing WIPMiFS 2003, Series of Metallurgy No 33.
[3] H. D y j a, S. M r ó z, D. R y d z, Politechnika Częstochowska, Prace Naukowe Wydziału Inżynierii Procesowej, Materiałowej i Fizyki Stosowanej, Seria: Metalurgia **33**, Częstochowa 2003.
[4] H. D y j a, S. M r ó z, A. M i l e n i n, Journal of Materials Processing Technology **153-154**, 100-107 (2004).
[5] FORGE3® Reference Guide Release 6.2, Sophia-Antipolis, November 2002.
[6] A. H e n z e l, T. S p i t t e l, Rasciet energosilovykh parametrov v processakh obrobotki metallov davlenijem, Metalurgija, Moskva 1982.
[7] S. M r ó z, Theoretical and experimental analysis of process of rolling bimetal bars, Ph.D. thesis, Częstochowa University of Technology 2002.
[8] S. M r ó z, K. J a g i e ł a, H. D y j a, Determination of the energy and power parameters during groove-rolling, Journal of Achievements in Materials and Manufacturing Engineering **22**, 2, 59-62 (2007).
[9] S. M r ó z, Modification of the roll pass design to the bar rolling process with longitudinal band separa-

tion, Archives of Metallurgy and Materials **54**, 597-605 (2009).

[10] S.J. P a w l a k, Austenite stability in the high strength metastable stainless steels, Journal of Achievements in Materials and Manufacturing Engineering **22**, 2, 91-94 (2007).

[11] S. S a w i c k i, Theoretical and experimental aspects of the bimetallic reinforcement bars steel – steel resistant to corrosion rolling process, Ph.D. thesis, Częstochowa University of Technology 2009.

[12] S. S a w i c k i, P. S z o t a, Numerical modeling of the process of bimetallic bar rolling in a three-high skew rolling mill, VIII International Scientific Conference entitled "New Technologies and Achievements in Metallurgy and Material Engineering 2007 Czestochowa", Conference Materials, Faculty of Process & Material Engineering and Applied Physics. Series of Metallurgy no. 48. s. 495-499. ISBN 978-83-7193-336-3.

[13] P. Š i m e č e k, D. H a j d u k, Prediction of mechanical properties of hot rolled steel products, Journal of Achievements in Materials and Manufacturing Engineering **20**, 395-398 (2007).

[14] I.H. S o n, Y.G. J i n, Y.T. I m, Finite element investigations of friction condition in equal channel angular extrusion, Journal of Achievements in Materials and Manufacturing Engineering **17**, 285-288 (2006).

[15] P. S z o t a, H. D y j a, Numerical modeling of the bimetallic reinforcement bar rolling process, Journal of Achievements in Materials and Manufacturing Engineering **25**, 1, 55-58 (2007).

[16] PN-ISO 6935-2 – Stal do zbrojenia betonu – Pręty żebrowane.

[17] PN-ISO 6935-2/AK – Stal do zbrojenia betonu – Pręty żebrowane - Dodatkowe wymagania stosowane w kraju.

Received: 20 March 2011.